Characterization of the megakaryocyte demarcation membrane system and its role in thrombopoiesis

Harald Schulze, Manav Korpal, Jonathan Hurov, Sang-We Kim, Jinghang Zhang, Lewis C. Cantley, Thomas Graf, and Ramesh A. Shivdasani

To produce blood platelets, megakaryocytes elaborate proplatelets, accompanied by expansion of membrane surface area and dramatic cytoskeletal rearrangements. The invaginated demarcation membrane system (DMS), a hallmark of mature cells, has been proposed as the source of proplatelet membranes. By direct visualization of labeled DMS, we demonstrate that this is indeed the case. Late in megakaryocyte ontogeny, the DMS gets loaded with PI-4,5-P_2, a phospholipid that is confined to plasma membranes in other cells. Appearance of PI-4,5-P_2 in the DMS occurs in proximity to PI-5-P-4-kinase α (PIP4Kα), and short hairpin (sh) RNA-mediated loss of PIP4Kα impairs both DMS development and expansion of megakaryocyte size. Thus, PI-4,5-P_2 is a marker and possibly essential component of internal membranes. PI-4,5-P_2 is known to promote actin polymerization by activating Rho-like GTPases and Wiskott-Aldrich syndrome (WASp) family proteins. Indeed, PI-4,5-P_2 in the megakaryocyte DMS associates with filamentous actin. Expression of a dominant-negative N-WASp fragment or pharmacologic inhibition of actin polymerization causes similar arrests in proplatelet formation, acting at a step beyond expansion of the DMS and cell mass. These observations collectively suggest a signaling pathway wherein PI-4,5-P_2 might facilitate DMS development and local assembly of actin fibers in preparation for platelet biogenesis. (Blood. 2006;107:3868-3875)

Introduction

Mammals synthesize blood platelets as functional cell particles within a precursor cell, the megakaryocyte (MK). Terminally differentiated MKs acquire a significantly polyploid DNA content and enlarge to 50 to 100 μm in diameter before releasing their platelet load. In the release phase, the MK cytoplasm converts into long branched protrusions, and disc-shaped platelets are assembled de novo within these proplatelet extensions.[1] Microtubule bundles form the core of each proplatelet, and their distal tips organize into the repetitively coiled structure of the platelet marginal band.[1-3] The actin cytoskeleton also participates actively in thrombopoiesis, judged mainly by the effects of inhibitors of actin polymerization on proplatelet morphology.[1,4-6] Although these studies reveal cytoskeletal aspects of thrombopoiesis, little is known about the corresponding regulation of nascent platelet membranes or how membrane and cytoskeletal morphogenesis are coordinated.

The conversion of a single MK into thousands of platelets is accompanied by a large increase in total surface area. MK ultrastructure reveals an abundant pool of cytoplasmic membranes that constitute the demarcation membrane system (DMS). By virtue of its origin in tubular invaginations of the plasma membrane, the DMS maintains continuity with the extracellular space,[7,8] and whole-cell patch-clamp recordings reveal the DMS to be a single electrophysiologic entity.[9] DMS functions, however, remain controversial, and its name recalls early theories on platelet biogenesis. Prior to proplatelet-based models of thrombopoiesis, nascent platelets were believed to assemble within the MK cytoplasm, partitioned or demarcated by these membranes.[10] Subsequently, the DMS was proposed to function instead as the membrane reservoir required to extend proplatelets.[11] This is an appealing idea that remains untested and also predicts that internal membranes evert in the course of platelet assembly.

Here, we provide direct evidence that the DMS is the source of proplatelet membranes. We show further that in anticipation of platelet release, these membranes acquire biochemical distinction in the form of harboring PI-4,5-P_2, a phospholipid that is usually associated with the plasma membrane. We suggest that PI-4,5-P_2 may accumulate through the enzymatic activity of the lipid kinase PI-5-P-4-kinase α (PIP4Kα), which is both enriched in MKs and required for expansion of the membrane and cell mass. Finally, PI-4,5-P_2 generated in the DMS associates with local assembly of a filamentous actin network, predominantly through the WASp-Arp2/3 pathway. Taken together, these results provide new insights into the structure and function of the DMS and suggest biochemical links between the membrane and cytoskeletal alterations that accompany terminal MK maturation and platelet release.

From the Dana-Farber Cancer Institute, Boston, MA; the Department of Medicine, Harvard Medical School, Boston, MA; the Beth Israel-Deaconess Medical Center, Boston, MA; and the Albert Einstein College of Medicine, Bronx, NY.

Submitted July 12, 2005; accepted January 12, 2006. Prepublished online as *Blood* First Edition Paper, January 24, 2006; DOI 10.1182/blood-2005-07-2755.

Supported by the National Institutes of Health (R01HL63143) and by a fellowship from the Deutsche Forschungsgemeinschaft (Schu1421/2-1) (H.S.).

H.S. and R.A.S. designed and performed the research and wrote the paper; M.K., J.H., S.-W.K., and J.Z. designed and performed the research; L.C.C. and T.G. designed the research.

An Inside *Blood* analysis of this article appears at the front of this issue.

The online version of this article contains a data supplement.

Reprints: Ramesh A. Shivdasani, Dana-Farber Cancer Institute, One Jimmy Fund Way, Boston, MA 02115; -mail: ramesh_shivdasani@dfci.harvard.edu.

The publication costs of this article were defrayed in part by page charge payment. Therefore, and solely to indicate this fact, this article is hereby marked "advertisement" in accordance with 18 U.S.C. section 1734.

Materials and methods

Mice, megakaryocyte culture, and proplatelet and platelet studies

GPIIb-EYFP knock-in mice were generated by conventional gene targeting (J.Z., Nicole Faust, Florencio Varas, and T.G., manuscript in preparation). All animal studies were approved by the Institutional Review Board at Dana-Farber Cancer Institute, Boston, MA. Fetal livers were recovered from mouse embryos between the 13th and 15th gestational days and cultured to expand megakaryocytes, as described previously.[12] Unless indicated otherwise, cells were separated on the fourth or fifth culture day over a 1.5% to 3% discontinuous bovine serum albumin (BSA) gradient to recover populations enriched or depleted for mature MKs. Washed cells were concentrated and processed for RNA or protein isolation. Electron microscopy of mouse bone marrow MKs[12] and isolation of mouse blood platelets[13] were performed as described previously. Proplatelets were monitored by phase-contrast microscopy of cells growing in suspension. For direct fluorescence microscopy and indirect immunofluorescence, blood platelets or 10^3 to 10^5 cultured MKs were cytocentrifuged onto poly L-lysine-coated coverslips or glass slides, respectively. MK preparations were fixed in 4% formaldehyde for 15 minutes, washed, permeabilized with PBS containing 0.5% Triton X-100 for 3 minutes, blocked with 3% goat serum in phosphate-buffered saline, and incubated with phycoerythrin-conjugated CD41 antibody (PharMingen, San Diego, CA) or Alexa Fluor594–conjugated phalloidin (Molecular Probes, Eugene, OR). Indirect immunofluorescence was performed using rabbit antiserum against PIP4Kα, rabbit antibody against Arp3 (Upstate Biotechnology, Lake Placid, NY), or mouse β-tubulin monoclonal antibody (clone 2-28-33; Sigma, St Louis, MO) and corresponding secondary goat antibodies conjugated with either FITC or Texas Red (Jackson Laboratories, Bar Harbor, ME). Cytochalasin D (Sigma) was dissolved in DMSO and added to MK cultures in 24-well tissue culture dishes at the indicated concentrations and time points.

Retrovirus production and megakaryocyte transduction

Intact or GFP-fused cDNAs were cloned into the pWZL plasmid prior to virus production in packaging cells, as described.[13] Briefly, 293 cells were cultured in DMEM supplemented with 10% FBS and transfected with 5 μg each of plasmids encoding *gag/pol*, vsv*G*, and pWZL constructs. Medium was exchanged after 16 hours, and viral supernatant was collected after 48 to 60 hours. The medium was filtered (0.45 μm) and either used immediately or stored at −80°C. Cells were isolated on day 2 of MK culture as described in the preceding section, and cultured for 16 to 24 hours in 1 mL DMEM containing 10% FBS, TPO (0.5% culture supernatant from a TPO producer cell line, as described previously[12]), 5 μg/mL polybrene (Sigma), and retroviral supernatants. Viral titers were not determined routinely, and supernatants were applied without modification when at least 5% of large cells (mature MKs) displayed GFP signals. Low-titer viral supernatants were concentrated by ultracentrifugation to achieve comparable infection rates; most supernatants gave infection rates between 5% and 60%, which was suitable for single-cell level analysis. Following exchange with fresh medium, MKs were cultured for 2 additional days.

For RNA interference, an oligonucleotide corresponding to the target sequence GGCTCGACAGTGGCTAGAGAA (nucleotides 640-660 of the murine type II PIP4Kα open reading frame) was cloned into the retroviral vector pMSCV/U6, which includes a puromycin-resistance cassette.[14] This construct or empty vector were transfected with EcoPak ecotropic retroviral packaging vector (gift of Benjamin Neel) into 293T cells. Culture supernatants were harvested after 48 hours and used to infect unseparated primary MK cultures for 24 hours on the second culture day, followed by selection in 2 μg/mL puromycin (Sigma). On day 5, MKs were separated over a BSA-step gradient, and the small-cell fraction was cultured further in TPO to produce a second wave of MKs, under continued selection in puromycin. Large MKs were separated again after 5 to 7 culture days. PIP4Kα levels were normal in the first MK wave (data not shown) and markedly reduced in the second (Figure 4A). Drug selection in suspension cultures, accompanied by cell expansion, precluded assessment of infection efficiency; sufficient cells were recovered in each experiment to permit biochemical, cytometric, and morphologic studies.

Plasmids

Constructs for the pleckstrin homology (PH) domain of phospholipase C (PLC) δ1 was kindly provided by Tamás Balla, Bethesda, MD. The cofilin and acidic (CA) domain from bovine WASp was a gift from Hervé Falet, Boston, MA. Other plasmids were generated in our laboratories.

Fluorescence microscopy

Immunostained coverslips were stained with DAPI, mounted with Fluoromount G (Southern Biotech, Birmingham, AL), and examined on an Olympus IX70 inverted fluorescence microscope (Olympus, Melville, NY) at room temperature. Images were acquired with a CM350 CCD camera (Applied Precision, Issaquah, WA) using 60× (Olympus PLAN-APO 1.40 NA, 0.10 mm WD) or 100× (PLAN-APO 1.40NA, 0.10 mm WD) oil objectives. Thirty to 50 cross-sections were taken at 0.2-μm spacing and deconvolved using 10 cycles with the Ratio method, using DeltaVision software (Applied Precision, Issaquah, WA). As the emission spectrum of EYFP overlaps with that of GFP, EYFP signals were acquired using GFP filter settings and represented in green. Three-dimensional video-enhanced reconstruction and contrast enhancement for some images were performed using the same software. Images were captured using Adobe Photoshop 7.0 software (Adobe, San Diego, CA).

Antiserum and immunoblot analysis

A naturally occurring PIP4Kα variant cDNA that encodes an enzyme lacking 59 N-terminal amino acids (Δ59N) was cloned into the pGEX-5 × 1 vector (Invitrogen, Carlsbad, CA). GST-fusion protein was expressed in the BL21 strain of *Escherichia coli*, purified using glutathione-conjugated Sepharose beads (Amersham, Uppsala, Sweden), and used to immunize New Zealand White rabbits (Sigma Genosys, The Woodlands, TX). Antibody specificity was assessed by immunoblotting. Cell populations enriched for MKs were lysed for 30 minutes on ice in buffer (20 mM HEPES, pH 7.4, 5 mM EDTA, 150 mM NaCl, 1% Triton X-100) supplemented with protease inhibitors (Sigma), and centrifuged at 15 000*g* at 4°C for 20 minutes. Protein (10 μg) per lane was resolved by sodium dodecyl sulfate–polyacrylamide gel electrophoresis (SDS-PAGE) and transferred onto PVDF membranes in transfer buffer (25 mM Tris-HCl, pH 7.5, 192 mM glycine, 20% methanol) at 100 V for 1 hour. The membrane was blocked in 50 mM Tris-HCl, pH7.5, 150 mM NaCl, 1% Tween-20 supplemented with 2% (wt/vol) BSA for 1 hour prior to addition of our generated antiserum (1:10 000). Washing, incubation with horseradish peroxidase–conjugated secondary antibody, and chemoluminescent detection were performed as described.[13]

Flow cytometry

MKs treated with drugs, shRNA, or corresponding controls were pelleted at the indicated times and incubated for 20 minutes in 100 μL PBS containing either FITC-conjugated CD41 antibody (clone MWReg30), phycoerythrin-conjugated CD61 antibody (clone 2C9.G2), or the corresponding isotype controls (all from Becton Dickinson, Franklin Lakes, NJ). Cells were washed and either scored manually for proplatelet formation (fraction of large cells elaborating ≥ 2 proplatelets) under phase-contrast microscopy or analyzed on a FACSCalibur (Becton Dickinson) flow cytometer for forward light scatter (FSC) after gating on single, live $CD41^+$ or $CD61^+$ cells.

Results

PI-4,5-P_2 is a lipid marker for the DMS

The invaginated membranes of the DMS are dispersed through most of the mature MK cytoplasm except for a cortical organelle-poor zone (Figure 1A). We studied a mouse strain ($EYFP^{ki}$) in

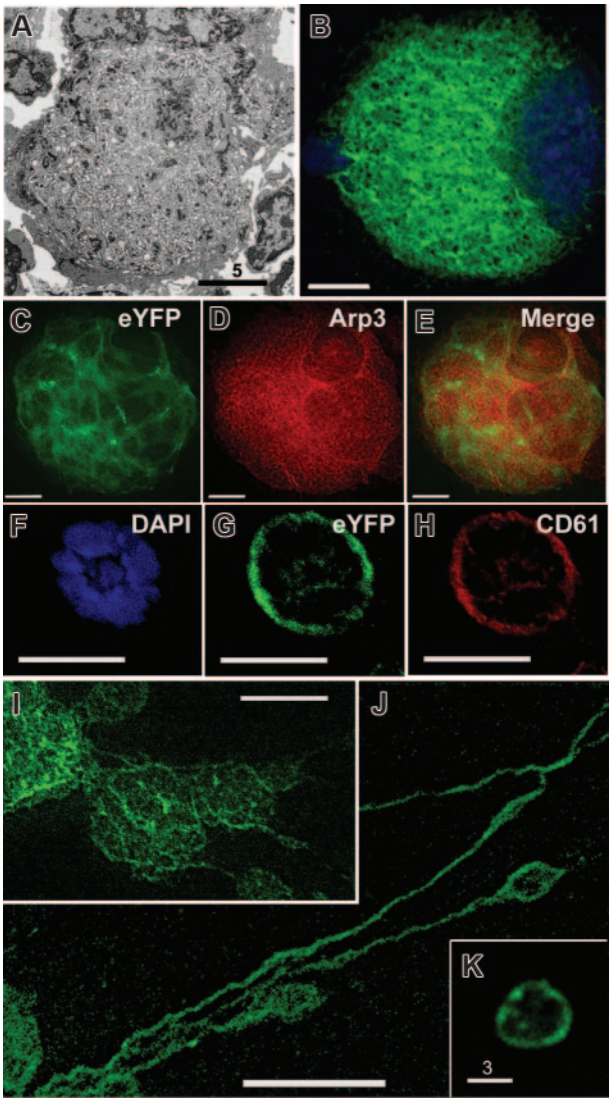

Figure 1. EYFP^{ki} MKs serve as reporters for the DMS. (A) Electron micrograph of a representative terminally differentiated MK, displaying abundant DMS that fills the cytoplasm except for the cell cortex. (B) MK derived from EYFP^{ki} mice, in which one *GPIIb* locus is replaced by modified (myristoyl-acceptor) EYFP cDNA, showing a fluorescent internal membrane system that corresponds to the morphology and distribution of the DMS. MK preparations centrifuged on cover slips were examined by fluorescence deconvolution microscopy; a central z-section is depicted. (C-E) Micrograph of a typical young EYFP^{ki} MK, with limited surface fluorescence; the cell is outlined (E) with CD61 antibody. (F-H) Costaining of advanced EYFP^{ki} MKs with Arp3 antibody (G) shows no correspondence between membranous EYFP signal and diffuse Arp3 staining. (I-K) Micrographs of EYFP^{ki} MKs in the process of elaborating proplatelets. Proplatelet membranes are contiguous with MK internal membranes, revealing directly that the latter provide the reservoir for proplatelet formation. (E) Peripheral blood platelets in EYFP^{ki} mice show surface fluorescence and further support a DMS origin for blood platelets. Scale bars: A, 5 μm; F-H, 10 μm; K, 3 μm; all others, 15 μm.

which the *GPIIb (CD41)* locus is replaced by cDNA encoding enhanced yellow fluorescent protein (EYFP); the reporter protein was modified by a C-terminal farnesylation site, which allows it to be incorporated in cellular membranes (J.Z., N. Faust, F. Varas, and T.G., manuscript in preparation). Young MKs showed low fluorescence that was confined to the cell periphery (Figure 1F-H). Fluorescence levels increased substantially in mature MKs (Figure 1B), judged by their size and nuclear lobularity, and the staining pattern was highly reminiscent of the DMS ultrastructure (Figure 1A). Indeed, the DMS is the only membrane system with the same mass and distribution as the observed EYFP localization. In cells with advanced differentiation, plasma-membrane signal was comparatively weak, and EYFP did not colocalized with the cytoplasmic and cytoskeletal marker Arp3 (Figure 1C-E), thus excluding the possibility that the fusion protein accumulates in the cytosol. Notably, the fluorescent internal membranes were contiguous with the full outline of emerging proplatelets (Figure 1I-J), and platelets circulating in EYFP^{ki} mice showed surface fluorescence (Figure 1K). These observations directly reveal the DMS as a reservoir for proplatelet and platelet membranes and suggest that EYFP^{ki} mice can serve as a tool to monitor the DMS.

Because the biochemistry of the DMS is obscure, we sought to identify molecules that might help elucidate its properties and serve as compartmental markers. Greater than 90% of the lipids in MK membranes consist of phosphatidylcholine, phosphatidylethanolamine, sphingomyelin, and phosphatidylserine[15]; much of the rest consists of the phosphatidylinositol (PI) group, wherein 7 species may be phosphorylated at specific positions.[16] Pleckstrin homology (PH) and Phox domains bind phospholipids with high affinity and specificity,[17,18] and fusion of these heterologous domains to enhanced green fluorescent protein (EGFP) permits interrogation of the phospholipid composition of cellular membranes. In particular, the PH domain derived from phospholipase Cδ1 (PLCδ1) binds predominantly to PI-4,5-P_2 in membranes, and a PH(PLCδ1)–EGFP fusion protein has been used to mark plasma membranes.[19,20] Indeed, in young MKs infected with PH(PLCδ1)–EGFP retrovirus, fluorescence was largely confined to the cell membrane (Figure 2A-D), where PI-4,5-P_2 expression is detected in other cell types.

As transduced MKs matured, however, the PH(PLCδ1)–EGFP probe showed a consistent and marked shift from the cell periphery into an internal compartment (Figure 2E). As we observed with EYFP^{ki} cells, the fluorescence pattern in cytologically advanced MKs strongly resembled the outline and features of the DMS (Figure 2F; also Supplemental Video S1, available on the *Blood* website by clicking on the Supplemental Materials link at the top of the online article). To better define the internal location of PH(PLCδ1)–marked membranes, we costained cells with CD41 antibody. CD41 staining outlined the whole cell, including the cortex (Figure 2E) and revealed that PI-4,5-P_2 distribution (Figure 2D) corresponds most closely to the DMS. A second MK internal membrane compartment, the rough endoplasmatic reticulum, which is histochemically identical to the platelet-dense tubular system,[21,22] is both less extensive and contiguous with the nuclear envelope. PH(PLCδ1)–EGFP did not show perinuclear concentration (Figure 2A-G), in agreement with the observation that less than 10% of cellular PI-4,5-P_2 resides in the ER in other cell types.[23] Thus, PI-4,5-P_2 accumulates in internal membranes, where it can serve to mark MK differentiation stages.

MKs lacking the transcription factor NF-E2 fail to form proplatelets and harbor a highly disorganized DMS.[12,24] Forced expression of PH(PLCδ1)–EGFP in NF-E2-null MKs resulted in abundant and uneven staining of cytoplasmic membranes (data not shown). Thus, MKs generate substantial PI-4,5-P_2 in the DMS prior to the step at which NF-E2 functions are required. Finally, in PH(PLCδ1)–EGFP–expressing MKs, proplatelet membranes were also fluorescent and contiguous with the stained internal membranes (Figure 2F-G). This observation supports our results with EYFP^{ki} MKs (Figure 1) and independently reveals the origin of proplatelets in the DMS.

Enzymatic origin of PI-4,5-P_2 at the DMS

Cells generate PI-4,5-P_2 by 2 alternative routes: a canonical pathway of PI-4-P phosphorylation by PI-4-P 5-kinases (type I) or

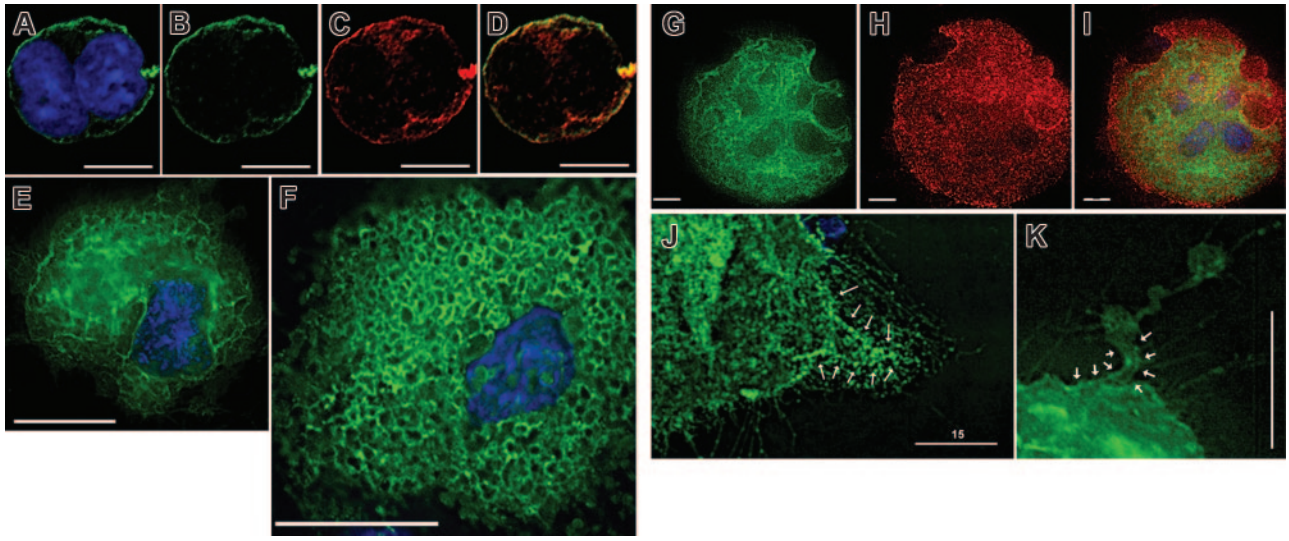

Figure 2. The megakaryocyte DMS accumulates PI-4,5-P_2 late in differentiation. MKs were retrovirally transduced with EGFP-tagged pleckstrin homology (PH) domain derived from phospholipase C (PLC)δ1, a specific probe for membrane-associated PI-4,5-P_2, and examined by fluorescence deconvolution microscopy. (A-D) In young MKs, only the plasma membrane shows PI-4,5-P_2 accumulation, as described for other cells. (A) EYFP merged with nuclear DAPI stain, (B) EYFP alone, (C) CD61 stain alone, (D) merger of EYFP and CD61 signals, showing overlap. (E) In MKs of advanced differentiation, internal membranes stain strongly with PH-PLCδ1. The cell-surface signal is weak, and the predominant staining is internal. (F) Continued cytologic maturation, judged by increased cell size and nuclear complexity, results in elaborate staining of internal membranes, which resemble the DMS as seen by electron microscopy and in $EYFP^{ki}$ mice, with virtual loss of cell-surface signal (see also Video S1). (G-I) Costaining of PH(PLCδ1)–EGFP–expressing MKs (G) with CD41 antibody (H), a surface and internal marker of MKs. Double staining (I) highlights the cortical absence of PI-4,5-P_2. (J-K) Proplatelets demonstrate PI-4,5-P_2 staining in contiguity (arrows) with internal membranes. Scale bars: A-D, 10 μm; E, F, J, K, 15 μm; G-I, 20 μm.

via type II kinases that phosphorylate PI-5-P at the 4 position.[25] The latter pathway may first convert PI-3-P into PI-3,5-P_2, which is subsequently cleaved to produce the PI-5-P substrate.[16,26,27] PI-5-P 4-kinase IIα (PIP4Kα) is expressed abundantly in the cytoplasm in the sibling erythrocyte and MK lineages[28,29]; in contrast to other PI kinases, it is excluded from the nucleus and plasma membrane in HeLa cells.[30,31] These features make PIP4Kα a good candidate for the enzyme that generates PI-4,5-P_2 in the DMS.

In platelets and MKs, PIP4Kα appears in 2 (51 kDa and 43 kDa) forms, as suggested for erythrocytes[32]; the smaller, less abundant form lacks 59 N-terminal amino acids, reflecting use of an alternative promoter and mRNA, which we have cloned from primary MKs and designate Δ59N-PIP4Kα (Figure S1A). Antisera that we raised against Δ59N-PIP4Kα also recognize the full-length protein (Figure 3A), and indirect immunofluorescence using these antibodies revealed cytoplasmic localization in MKs (Figure 3B). To confirm this result, we used EGFP fusion proteins. Retroviral expression of EGFP-tagged full-length PIP4Kα was toxic to cultured MKs, but surviving cells showed exclusively cytoplasmic fluorescence (data not shown). As enzymatic activity of the Δ59N form is comparable to that of the full-length protein (Figure S1B), we used this nontoxic natural variant to refine subcellular localization. EGFP-Δ59N-PIP4Kα concentrated at DMS-like internal membranes, sparing both the membrane-depleted periphery and the plasma membrane (Figure 3C). This distribution was confirmed by costaining the cells with CD41 antibody (data not shown). Although it is formally possible that the Δ59N variant is regulated differently, these data suggest that PIP4Kα resides in the vicinity of the DMS and of its product PI-4,5-P_2. In contrast, some PI4P 5-kinases (PIP5Kα and PIP5Kβ) are also expressed in MKs, but neither of these enzymes colocalizes with the DMS; both enzymes appear mainly in the cell periphery (Figure 3D-E; Chen et al[33]) and thus are not suitably positioned to produce PI-4,5-P_2 in the DMS. Taken together, these findings support the candidacy of PIP4Kα as the pertinent enzyme.

To assess PIP4Kα function, we used retroviral infection to introduce sequence-specific short hairpin (sh) RNAs into primary MKs. Preliminary studies in cultured fibroblasts indicated prolonged stability of the target protein and the need for several days of shRNA exposure to abrogate expression (data not shown). Although this duration exceeds the MK lifespan, hematopoietic-cell cultures yield successive waves of megakaryopoiesis, albeit with reduced proplatelet formation at each wave. We could deplete PIP4Kα in the second wave (Figure 4A) and eliminate it by the third wave; loss of PIP4K with the applied shRNA was selective for the α protein and spared the β isoform (Figure 4B). Cells treated with empty vector generated MKs similar to untreated cells,

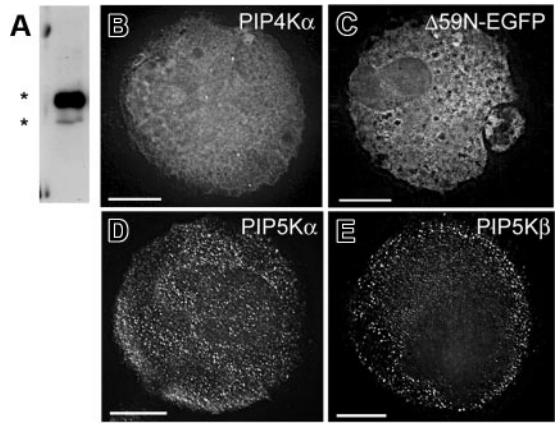

Figure 3. PIP4Kα resides in or near MK internal membranes. (A) Immunoblot of cultured primary mouse MKs with a specific PIP4Kα antibody detects expression of full-length and truncated (Δ59N) splice variants (asterisks). (B) Indirect immunofluorescence with PIP4Kα antiserum. A representative z-section is shown after deconvolution microscopy. (C) EGFP-fused Δ59N-PIP4Kα was forcibly expressed in primary MKs, and serial z-sections from fluorescence deconvolution microscopy revealed internal (not peripheral or nuclear) localization, in a membrane-associated distribution that resembles the DMS. (D-E) Cultured MKs stained with antibodies against type I PIP kinases reveal that the cellular distribution of these enzymes differs from that of PIP4Kα. Single z-sections are shown after deconvolution. Scale bars: 15 μm.

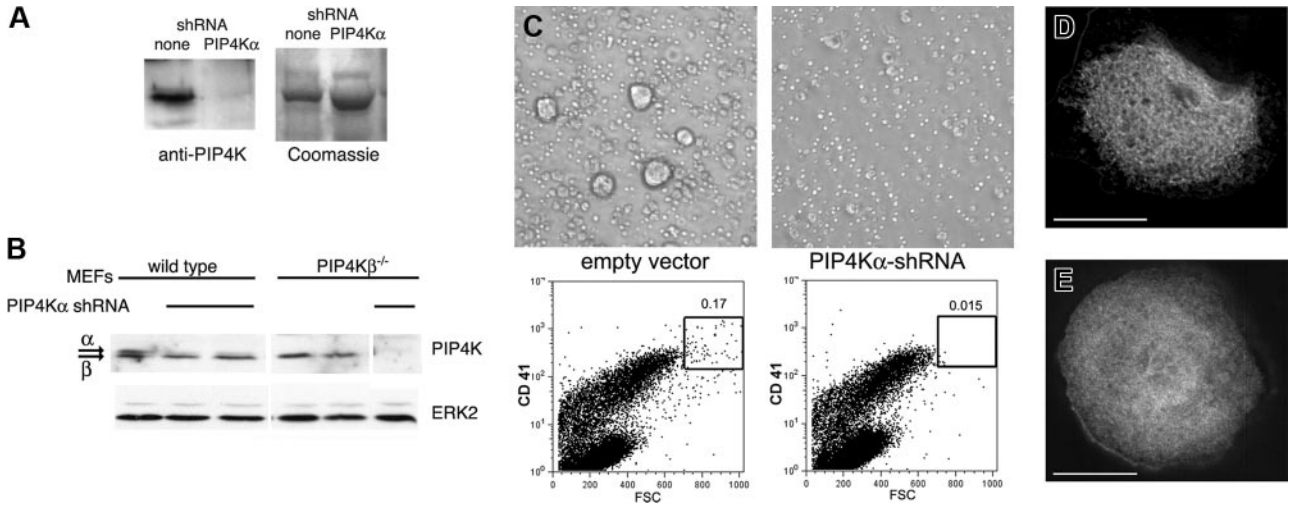

Figure 4. PIP4Kα shRNA induces absence of large MKs. (A) Mouse fetal liver cultures were treated with retroviruses that drive expression of PIP4Kα-specific shRNA and selected in puromycin. Cell fractions enriched for MK progenitors were isolated on day 5 and cultured further under drug selection. MKs from the ensuing (second) wave were used to prepare protein lysates and immunoblotted with PIP4Kα antiserum to reveal substantial down-regulation of the target protein compared with controls (empty vector). Protein loading was verified by Coomassie blue staining (right; only part of the gel is shown). (B) Selectivity of PIP4Kα shRNA. The PIP4Kα antibody recognizes PIP4Kα better than PIP4Kβ. Mouse embryonic fibroblasts (MEFs) from wild-type or PIP4Kβ-nullizygous mice were treated with the same PIP4Kα shRNA. Both kinase isoforms are present in wild-type MEFs, whereas PIP4K$\beta^{-/-}$ MEFs only express PIP4Kα. The shRNA specifically depletes PIP4Kα without affecting the PIP4Kβ isoform. (C) Progenitor fractions were monitored for MK differentiation. PIP4Kα shRNA-treated cells failed to develop into the largest MKs, as judged by both phase-contrast light microscopy (top) and 2-parameter flow cytometry (bottom) for forward light scatter (x-axis; FSC) and surface CD41 (y-axis). (D-E) Similar studies were conducted with EYFP^{ki} MKs. Representative micrographs show typical membrane staining of MKs treated with control (empty) virus (D), whereas in PIP4Kα-depleted MKs (E), the cytoplasmic fluorescent signal is uniform and lacks definition corresponding to internal membranes. Scale bars, 15 μm.

whereas cultures treated with PIP4Kα shRNA showed near absence of large, cytologically mature MKs (Figure 4C). In 3 independent experiments, both phase-contrast light microscopy and 2-parameter flow cytometry for surface GPIIb (CD41) expression (as a MK lineage marker) and forward light scatter (FSC, a measure of cell volume) revealed selective loss of the largest (CD41$^+$, FSC^{high}) MKs. Cell viability, as judged by trypan blue dye exclusion, was unaffected (data not shown). Although less mature, intermediate-size MKs appeared in normal numbers (Figure 4C), we did not evaluate membrane morphology or phenotypes in these cells.

These results suggest a specific requirement for PIP4Kα in terminal maturation of CD41$^+$ MKs. To assess whether absence of PIP4Kα affects DMS structure, we applied the shRNA treatment to MKs from EYFP^{ki} mice and examined cells by deconvolution fluorescence microscopy. The target cell population is absent in the third wave of megakaryopoiesis (Figure 4C). However, in the preceding wave, when PIP4Kα is considerably reduced, staining of the EYFP^{ki} MK cytoplasm is diffuse, suggestive of notable membrane loss or disorganization (Figure 4D-E). These results directly implicate PIP4Kα in the expansion of cell size and the organization of the DMS and raise the possibility that the 2 processes may be functionally coupled.

Relation of the DMS to MK maturation

Having observed that the DMS loads with PI-4,5-P_2 before forming proplatelets, we investigated the possible consequences of this change in membrane phospholipids. PI-4,5-P_2 has multiple known functions, one of which is to trigger actin polymerization.[34-36] Indeed, in mature EYFP^{ki} MKs stained with fluorescent phalloidin, actin filaments colocalize with many portions of the DMS (data not shown). Similarly, in MKs infected with PH(PLCδ1)–EGFP retrovirus and correlating with the degree of cytologic maturity, we observed significant colocalization of the DMS and F-actin (Figure 5A-C; the example illustrates merger of fluorescent signals, mainly at one cell pole). Juxtaposition of PI-4,5-P_2–positive cell membranes and actin filaments is preserved in proplatelet extensions (Figure 5D-F). When invaginated internal membranes are extruded as proplatelets, they must turn inside-out, and proplatelet extensions are replete with filamentous actin.[1,37] These data and considerations led us to explore the possibility that accumulation of PI-4,5-P_2 in the DMS may stimulate actin polymerization in mature MKs.

Rho-family GTPases are especially linked to PI-4,5-P_2, which activates Rho-dependent kinases to induce actin stress fibers[38] and regulates Rac1-dependent actin assembly.[39] PI-4,5-P_2–dependent signaling from these GTPases to the Arp2/3 actin-nucleating complex is mediated by the Wiskott-Aldrich syndrome protein (WASp) family.[40] To address whether DMS-associated actin assembly occurs through this pathway, we exploited the dominant inhibitory function of an isolated C-terminal WASp CA (cofilin-binding and acidic) domain, which antagonizes actin-related functions by sequestering Arp2/3.[41,42] On retroviral transduction of primary MKs, an N-WASp CA fragment fused to EGFP colocalized substantially with Arp3 (Figure 5G-I), suggesting that its action occurs as expected. Punctate phalloidin staining in infected cells (Figure 5J) contrasts with the typically filamentous pattern and confirms the anticipated interference with actin assembly. WASp-CA-EGFP did not affect MK size, but compared with the EGFP (Figure 5K) or untreated (data not shown) controls, it inhibited dramatically the ability of MKs to elaborate proplatelets. Infected cells increased in size, showed multilobed nuclei, and extended occasional proplatelets (Figure 5L and inset), thus excluding severe cytotoxicity as the basis for arrested differentiation. Actin assembly is important at several steps in thrombopoiesis: initial protrusion of proplatelets and subsequent branching of individual proplatelet strands.[1,5,6] WASp-CA appears to block the first of these steps, which suggests that WASp-Arp2/3–dependent actin assembly is an essential and early event in proplatelet formation (PPF).

Taken together, our results are consistent with a signaling pathway wherein PI-4,5-P_2 in the DMS activates the WASp-Arp2/3 complex and thereby nucleates F-actin in preparation for platelet

release. To test the predictions of this model, we inhibited actin polymerization with cytochalasin D (cytoD). If actin assembly is essential early in proplatelet morphogenesis, the presence of cytoD should reduce PPF when the first wave of cultured primary MKs terminates maturation. In contrast, later exposure to cytoD might inhibit strand branching but should not reduce the number of proplatelet-producing cells. This is exactly what we observed (Figure 5M). Application of cytoD on or before culture day 2.5 nearly eliminated PPF, measured at its usual peak on day 4. Proplatelet numbers were unaffected if cytoD was applied on or after day 3, when the drug adversely influenced proplatelet morphology and branching as expected. CytoD-induced disruption of F-actin was confirmed by phalloidin staining and did not impair cell survival (data not shown). A second prediction is that, unlike manipulations that affect the DMS, cytoD treatment should preserve both cell volume and the morphology of internal membranes. Indeed, cytoD did not alter DMS structure in $EYFP^{ki}$ MKs (Figure 5N). Moreover, in contrast to the effects on PPF (Figure 5M) and to the effects of PIP4Kα shRNA on cell dimensions, we observed little difference in cell size distribution between MKs treated with cytoD on culture day 2.5 or thereafter (Figure 5O).

Discussion

At the conclusion of their maturation, MKs elaborate remarkably dynamic proplatelets that can extend for several millimeters. To support de novo assembly of thousands of platelets, MKs must coordinate numerous interactions between membrane, cytoskeletal, and signaling systems. Whereas some of the cytoskeletal changes associated with thrombopoiesis are known, the role of cellular membranes and their resident phospholipids is poorly understood. We show that PI-4,5-P_2 is a prominent marker lipid for internal membranes in mature MKs and identify the DMS as the origin of the proplatelet and platelet surface. Our studies suggest a model wherein MK-expressed lipid kinases, possibly PIP4Kα in particular, generate abundant PI-4,5-P_2 at the DMS concurrent with terminal differentiation. We also present data in support of a function for PI-4,5-P_2 accumulation in the DMS: to trigger cytoplasmic actin polymerization via the WASp/WAVE pathway.

Ultrastructural studies of the DMS reveal that it invaginates from the plasma membrane and presents profiles of fenestrated tubules and cisternae.[7,9-11] Reflecting the extensive invagination, the specific membrane capacitance per unit peripheral surface area in primary rat MKs, 8 to 9 μF/cm^2, exceeds that in most other cell types and increases 1.4-fold per doubling of spherical surface area.[9] These measurements suggest that MK enlargement is inherently coupled to development of the DMS and agree with observations that DMS abundance correlates with MK diameter.[7] Using $EYFP^{ki}$ cells and EGFP-PH(PLCδ1)–stained MKs, we show that the DMS directly provides the abundant membrane reserve required for proplatelet formation. Our studies, however, leave 2 possibilities open: (1) DMS segments may evert through an intact plasma membrane, akin to extrusion of toothpaste from a tube; or (2) the immediate origin of proplatelets may be in the plasma membrane. In this scenario, the DMS would provide a steady source of additional membrane, as in balls of knitting yarn, whereby yarn drawn from the edge is continuously replenished from internal material.

In any case, the side of the invaginated DMS that faces the extracellular space must emerge as the proplatelet surface, much

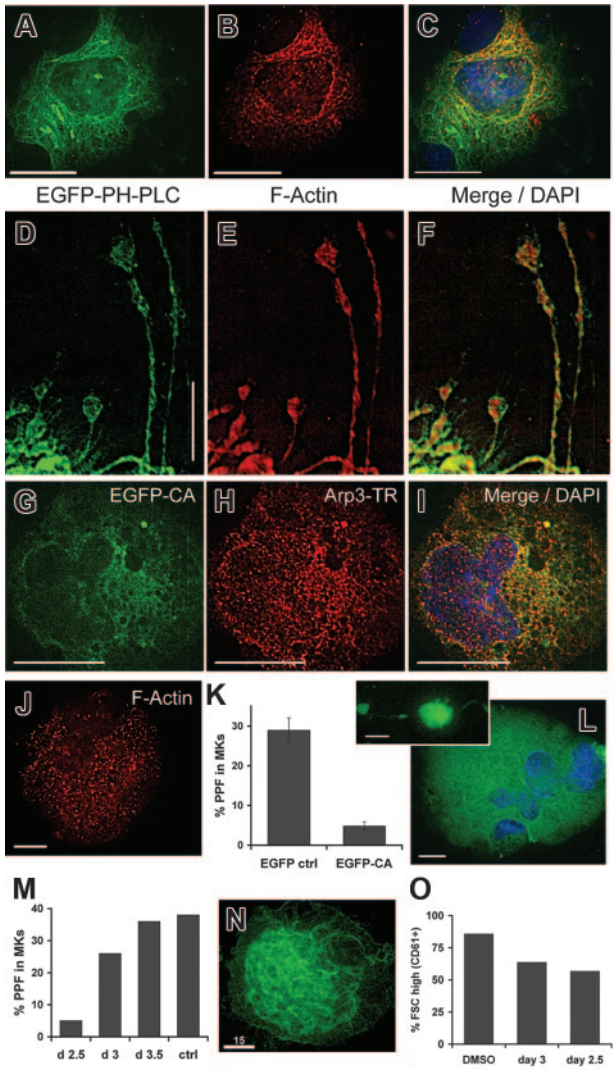

Figure 5. Actin fibers assemble near MK internal membranes and are required for proplatelet formation. (A-F) Wild-type MKs infected with PH(PLCδ1)–EGFP retrovirus were fixed, permeabilized, and labeled with Texas Red–phalloidin and DAPI nuclear stain on culture day 4. A central z-section in panel A reveals internal, PI-4,5-P_2–containing membranes. Phalloidin-stained actin filaments appear in a reticular network that colocalizes partially with PH(PLCδ1)–EGFP at one cell pole (B), as judged by merger of fluorescent signals (C). PI-4,5-P_2–positive proplatelet membranes also associate closely with actin filaments, suggesting continuity of the spatial relationship established in the cell body (D-F). (G-I) MKs were infected with retroviruses to express EGFP-tagged N-WASp CA domain, and infected cells were identified by fluorescence microscopy. The tagged CA domain colocalizes extensively with Texas Red–labeled Arp3, as shown by the merger of fluorescent signals. (J) Phalloidin staining of WASp-CA–expressing cells confirms disruption of actin filaments, which also failed to colocalize with the EGFP-CA fragment (data not shown). (K) EGFP-CA and control retroviruses were used to infect MKs on culture day 2, and proplatelet formation was scored on day 4. Expression of the isolated CA domain substantially reduced proplatelet formation. Results are averaged from 3 independent experiments, and are presented with standard deviations (error bars). (L) WASP-CA–infected MKs are large, have multilobed nuclei, and extend rare proplatelets (inset), findings that argue against general toxicity. (M) Proplatelet formation by cytochalasin D–treated MKs on culture day 4. Results show the effects of introducing cytoD into MK cultures between days 2.5 and 3.5 and are averaged over 3 independent experiments. Ctrl indicates DMSO treatment for 2.5 days. (N) Representative $EYFP^{ki}$ MK treated with cytoD on culture day 2, showing the characteristically elaborate internal membrane structure. (O) Cells treated with DMSO (control) or with 0.2 μM cytoD on culture days 2.5 or 3 were assessed for cell size on day 4. The fraction of FSC^{high} MKs ($CD61^+$ cells) is shown from 2 independent experiments. MKs were reduced slightly in size but showed little difference over the same interval in which proplatelet formation (M) was notably inhibited. Scale bars: A-I, N, 15 μm; J, L, 10 μm.

like the turning of a glove inside out. Contents on the cytoplasmic side include the contents of future platelets and factors responsible for proplatelet morphogenesis such as oriented microtubule bundles. In one of the last visible events in the MK-cell body, dispersed microtubules reorganize in thick bundles at the cell cortex and enable pseudopod formation.[1] At or about the same time, portions of the DMS dilate considerably and migrate into the cell periphery,[5,37] presumably to prepare for microtubule-powered eversion as proplatelets. Our data raise the possibility that the protrusive force for internal DMS migration, distinct from subsequent elongation of proplatelets, might rely on actin fibers that assemble at the DMS cytoplasmic face in response to local PI-4,5-P_2 signaling. This model is consistent with the demonstrated role of PI-4,5-P_2 signaling in a range of membrane motility functions, including ruffle formation, endocytosis, membrane traffic, and phagocytosis.[43-48] However, models of thrombopoiesis are inferred largely from still images of MKs, and current understanding of MK morphogenesis remains sketchy. DMS movement and eversion are especially mysterious acts, as are the role and fate of the MK plasma membrane. deBotton et al[49] have identified phosphatidylserine as a membrane lipid present on MK but not proplatelet surfaces. The sum of evidence thus suggests that internal MK membranes acquire distinctive biochemical and functional properties, whereas parts of the cell bounded by the plasma membrane are destined to degenerate.

Our results help construct a rough outline that divides terminal MK differentiation into sequential phases. DMS invagination occurs after endomitosis is completed, and expansion of the DMS mass and synthesis of platelet granules occur simultaneously.[7,50] Despite the origin of the DMS in the plasma membrane, it does not appear initially to contain much PI-4,5-P_2, which the (PH)PLCδ1 beacon reveals only in the plasma membrane (Figure 2). Subsequent loading of the DMS with PI-4,5-P_2 correlates with subcellular localization of PIP4Kα, an enzyme that is required to increase MK size (Figure 4C) and stabilize DMS membranes (Figure 4D-E). These correlative observations suggest a causative effect that will need to be established in future genetic and molecular studies. Subsequently, actin filaments assemble near the DMS (Figure 5A-C) and are required after the cell achieves its terminal proportions: cytochalasin D and the N-WASp CA fragment interfere with proplatelet formation but not with MK enlargement (Figure 5K-O). We suggest that PI-4,5-P_2 might serve as a molecular bridge between these steps and transmit one of several possible signals to trigger actin assembly. Finally, microtubules are mobilized to transport organelles and to extend proplatelets,[1,5] a process that is largely independent of actin, although proplatelets contain long arrays of actin filaments.[1,37] Each of these steps represents a potential target for interference, and it should soon be possible to consider thrombopoietic disorders according to the specific stage in MK maturation that is affected.

Distinctive PI species usually mark different cellular membrane compartments; PI-3-P and PI-3,5-P_2, for example, are found on endosomes and internal vesicles, respectively (reviewed in Roth[51]). The bulk of cellular PI-4,5-P_2 is usually present at the plasma membrane, with less than 10% detected in the Golgi and endoplasmic reticulum,[23] and may be produced in a synthetic pathway via PI-4-P. The corresponding lipid kinases accordingly localize at the plasma membrane and, to a lesser degree, in nuclear speckles. These type I kinases may account for much of the cellular PIP_2 turnover in MKs. However, as they are present mainly in the cell periphery but not in the DMS (Figure 3D-E), and the plasma membrane loses PIP_2 over time, we suggest an additional role for type II kinases, which use PI-5-P as the substrate to generate PI-4,5-P_2. Indeed, PIP4Kα associates largely with internal MK membranes, and deficiency of the enzyme impairs expansion of DMS and cell mass. The extended β-sheet structure of a homologous enzyme, PIP4Kβ, presents an enormous surface area for membrane interactions.[52] By analogy, PIP4Kα likely associates with the considerable DMS mass to increase its PI-4,5-P_2 content concurrent with cell maturation.

Extension of branched actin filaments occurs through Arp2/3-containing complexes and WASp/WAVE proteins,[36,53,54] which are expressed abundantly in MKs.[55] PI-4,5-P_2 enhances WASp binding to Arp2/3[36,56,57] and its accumulation on the mature DMS could trigger Rho-family GTPases to activate WASp/WAVE proteins locally and stimulate actin fiber assembly. Although our results imply that these are essential events to initiate PPF, actin is required again at a later step, when cytochalasins reduce or eliminate proplatelet branching.[1,6] Furthermore, DMS-associated actin assembly probably represents one of many stimuli for PPF, because thrombopoiesis is blocked in NF-E2–deficient MKs even though their DMS accumulates both PI-4,5-P_2 and associated actin fibers (data not shown). For example, actin assembly in maturing MKs responds to external signals transmitted through integrins and other glycoprotein receptors.[58]

In summary, we show that the DMS is the source of proplatelet and platelet membranes and explore some of its characteristics. These studies, conducted exclusively in primary MKs, the only source of bona fide platelets, advance understanding of how MK membranes and cytoskeleton may be coordinated for platelet assembly and release.

Acknowledgments

We thank Tamás Balla, Hervé Falet, and Tom Roberts for PH-PLCδ1, WASP-CA, and retroviral expression plasmids, respectively; Ben Neel for the gift of ecotropic retroviral packaging vector; Andreas Krueger for help with flow cytometry; Katja Lamia for PIP kinase assays; and John Hartwig for critical review of the manuscript.

R.A.S. is a Scholar of the Leukemia and Lymphoma Society.

References

1. Italiano JE Jr, Lecine P, Shivdasani RA, Hartwig JH. Blood platelets are assembled principally at the ends of proplatelet processes produced by differentiated megakaryocytes. J Cell Biol. 1999;147:1299-1312.
2. Kenney DM, Linck RW. The cytoskeleton of unstimulated blood platelets: structure and composition of the isolated marginal microtubular band. J Cell Sci. 1985;78:1-22.
3. Schwer HD, Lecine P, Tiwari S, Italiano JE Jr, Hartwig JH, Shivdasani RA. A lineage-restricted and divergent beta-tubulin isoform is essential for the biogenesis, structure and function of blood platelets. Curr Biol. 2001;11:579-586.
4. Leven RM, Nachmias VT. Cultured megakaryocytes: changes in the cytoskeleton after ADP-induced spreading. J Cell Biol. 1982;92:313-323.
5. Tablin F, Castro M, Leven RM. Blood platelet formation in vitro: the role of the cytoskeleton in megakaryocyte fragmentation. J Cell Sci. 1990; 97(Pt 1):59-70.
6. Rojnuckarin P, Kaushansky K. Actin reorganization and proplatelet formation in murine megakaryocytes: the role of protein kinase calpha. Blood. 2001;97:154-161.
7. Behnke O. An electron microscope study of the megacaryocyte of the rat bone marrow, I: the development of the demarcation membrane system and the platelet surface coat. J Ultrastruct Res. 1968;24: 412-433.
8. Shaklai M, Tavassoli M. Demarcation membrane

system in rat megakaryocyte and the mechanism of platelet formation: a membrane reorganization process. J Ultrastruct Res. 1978;62:270-285.

9. Mahaut-Smith MP, Thomas D, Higham AB, et al. Properties of the demarcation membrane system in living rat megakaryocytes. Biophys J. 2003;84:2646-2654.
10. Tavassoli M. Megakaryocyte–platelet axis and the process of platelet formation and release. Blood. 1980;55:537-545.
11. Radley JM, Haller CJ. The demarcation membrane system of the megakaryocyte: a misnomer? Blood. 1982;60:213-219.
12. Lecine P, Villeval JL, Vyas P, Swencki B, Xu Y, Shivdasani RA. Mice lacking transcription factor NF-E2 provide in vivo validation of the proplatelet model of thrombocytopoiesis and show a platelet production defect that is intrinsic to megakaryocytes. Blood. 1998;92:1608-1616.
13. Schulze H, Korpal M, Bergmeier W, Italiano JE Jr, Wahl SM, Shivdasani RA. Interactions between the megakaryocyte/platelet-specific beta1 tubulin and the secretory leukocyte protease inhibitor SLPI suggest a role for regulated proteolysis in platelet functions. Blood. 2004;104:3949-3957.
14. Devroe E, Silver PA. Retrovirus-delivered siRNA. BMC Biotechnol. 2002;2:15.
15. Schick BP, Schick PK, Chase PR. Lipid composition of guinea pig platelets and megakaryocytes: the megakaryocyte as a probable source of platelet lipids. Biochim Biophys Acta. 1981;663:239-248.
16. Tolias KF, Cantley LC. Pathways for phosphoinositide synthesis. Chem Phys Lipids. 1999;98:69-77.
17. Dowler S, Currie RA, Campbell DG, et al. Identification of pleckstrin-homology-domain-containing proteins with novel phosphoinositide-binding specificities. Biochem J. 2000;351:19-31.
18. Sato TK, Overduin M, Emr SD. Location, location, location: membrane targeting directed by PX domains. Science. 2001;294:1881-1885.
19. Varnai P, Balla T. Visualization of phosphoinositides that bind pleckstrin homology domains: calcium- and agonist-induced dynamic changes and relationship to myo-[3H]inositol-labeled phosphoinositide pools. J Cell Biol. 1998;143:501-510.
20. Brown FD, Rozelle AL, Yin HL, Balla T, Donaldson JG. Phosphatidylinositol 4,5-bisphosphate and Arf6-regulated membrane traffic. J Cell Biol. 2001;154:1007-1017.
21. Breton-Gorius J, Guichard J. Ultrastructural localization of peroxidase activity in human platelets and megakaryocytes. Am J Pathol. 1972;66:277-293.
22. Daimon T, Gotoh Y. Cytochemical evidence of the origin of the dense tubular system in the mouse platelet. Histochemistry. 1982;76:189-196.
23. Watt SA, Kular G, Fleming IN, Downes CP, Lucocq JM. Subcellular localization of phosphatidylinositol 4,5-bisphosphate using the pleckstrin homology domain of phospholipase C delta1. Biochem J. 2002;363:657-666.
24. Shivdasani RA, Rosenblatt MF, Zucker-Franklin D, et al. Transcription factor NF-E2 is required for platelet formation independent of the actions of thrombopoietin/MGDF in megakaryocyte development. Cell. 1995;81:695-704.
25. Rameh LE, Tolias KF, Duckworth BC, Cantley LC. A new pathway for synthesis of phosphatidylinositol-4,5-bisphosphate. Nature. 1997;390:192-196.
26. Shisheva A. PIKfyve: the road to PtdIns 5-P and PtdIns 3,5-P(2). Cell Biol Int. 2001;25:1201-1206.
27. Schaletzky J, Dove SK, Short B, Lorenzo O, Clague MJ, Barr FA. Phosphatidylinositol-5-phosphate activation and conserved substrate specificity of the myotubularin phosphatidylinositol 3-phosphatases. Curr Biol. 2003;13:504-509.
28. Ling LE, Schulz JT, Cantley LC. Characterization and purification of membrane-associated phosphatidylinositol-4-phosphate kinase from human red blood cells. J Biol Chem. 1989;264:5080-5088.
29. Divecha N, Truong O, Hsuan JJ, Hinchliffe KA, Irvine RF. The cloning and sequence of the C isoform of PtdIns4P 5-kinase. Biochem J. 1995;309(Pt 3):715-719.
30. Ciruela A, Hinchliffe KA, Divecha N, Irvine RF. Nuclear targeting of the beta isoform of type II phosphatidylinositol phosphate kinase (phosphatidylinositol 5-phosphate 4-kinase) by its alpha-helix 7. Biochem J. 2000;346(Pt 3):587-591.
31. Hinchliffe KA, Ciruela A, Letcher AJ, Divecha N, Irvine RF. Regulation of type IIalpha phosphatidylinositol phosphate kinase localisation by the protein kinase CK2. Curr Biol. 1999;9:983-986.
32. Bazenet CE, Ruano AR, Brockman JL, Anderson RA. The human erythrocyte contains two forms of phosphatidylinositol-4-phosphate 5-kinase which are differentially active toward membranes. J Biol Chem. 1990;265:18012-18022.
33. Chen X, Wang Y, Bach TL, et al. Mice lacking PIP5Kβ or PIP5Kγ have unique cytoskeletal changes within their megakaryocytes and platelets [abstract 380]. Blood. 2005;106:115a.
34. Janmey PA. Phosphoinositides and calcium as regulators of cellular actin assembly and disassembly. Annu Rev Physiol. 1994;56:169-191.
35. Ma L, Cantley LC, Janmey PA, Kirschner MW. Corequirement of specific phosphoinositides and small GTP-binding protein Cdc42 in inducing actin assembly in Xenopus egg extracts. J Cell Biol. 1998;140:1125-1136.
36. Rohatgi R, Ma L, Miki H, et al. The interaction between N-WASP and the Arp2/3 complex links Cdc42-dependent signals to actin assembly. Cell. 1999;97:221-231.
37. Cramer EM, Norol F, Guichard J, et al. Ultrastructure of platelet formation by human megakaryocytes cultured with the Mpl ligand. Blood. 1997;89:2336-2346.
38. Yamamoto M, Hilgemann DH, Feng S, et al. Phosphatidylinositol 4,5-bisphosphate induces actin stress-fiber formation and inhibits membrane ruffling in CV1 cells. J Cell Biol. 2001;152:867-876.
39. Tolias KF, Hartwig JH, Ishihara H, Shibasaki Y, Cantley LC, Carpenter CL. Type Ialpha phosphatidylinositol-4-phosphate 5-kinase mediates Rac-dependent actin assembly. Curr Biol. 2000;10:153-156.
40. Rozelle AL, Machesky LM, Yamamoto M, et al. Phosphatidylinositol 4,5-bisphosphate induces actin-based movement of raft-enriched vesicles through WASP-Arp2/3. Curr Biol. 2000;10:311-320.
41. Miki H, Miura K, Takenawa T. N-WASP, a novel actin-depolymerizing protein, regulates the cortical cytoskeletal rearrangement in a PIP2-dependent manner downstream of tyrosine kinases. EMBO J. 1996;15:5326-5335.
42. Suzuki T, Miki H, Takenawa T, Sasakawa C. Neural Wiskott-Aldrich syndrome protein is implicated in the actin-based motility of Shigella flexneri. EMBO J. 1998;17:2767-2776.
43. Honda A, Nogami M, Yokozeki T, et al. Phosphatidylinositol 4-phosphate 5-kinase alpha is a downstream effector of the small G protein ARF6 in membrane ruffle formation. Cell. 1999;99:521-532.
44. Sechi AS, Wehland J. The actin cytoskeleton and plasma membrane connection: PtdIns(4,5)P(2) influences cytoskeletal protein activity at the plasma membrane. J Cell Sci. 2000;113(Pt 21):3685-3695.
45. Botelho RJ, Teruel M, Dierckman R, et al. Localized biphasic changes in phosphatidylinositol-4,5-bisphosphate at sites of phagocytosis. J Cell Biol. 2000;151:1353-1368.
46. Martin TF. PI(4,5)P(2) regulation of surface membrane traffic. Curr Opin Cell Biol. 2001;13:493-499.
47. Pollard TD, Borisy GG. Cellular motility driven by assembly and disassembly of actin filaments. Cell. 2003;112:453-465.
48. Huang S, Lifshitz L, Patki-Kamath V, Tuft R, Fogarty K, Czech MP. Phosphatidylinositol-4,5-bisphosphate-rich plasma membrane patches organize active zones of endocytosis and ruffling in cultured adipocytes. Mol Cell Biol. 2004;24:9102-9123.
49. deBotton S, Sabri S, Daugas E, et al. Platelet formation is the consequence of caspase activation within megakaryocytes. Blood. 2002;100:1310-1317.
50. Bentfeld-Barker ME, Bainton DF. Ultrastructure of rat megakaryocytes after prolonged thrombocytopenia. J Ultrastruct Res. 1977;61:201-214.
51. Roth MG. Phosphoinositides in constitutive membrane traffic. Physiol Rev. 2004;84:699-730.
52. Rao VD, Misra S, Boronenkov IV, Anderson RA, Hurley JH. Structure of type IIbeta phosphatidylinositol phosphate kinase: a protein kinase fold flattened for interfacial phosphorylation. Cell. 1998;94:829-839.
53. Rohatgi R, Ho HY, Kirschner MW. Mechanism of N-WASP activation by CDC42 and phosphatidylinositol 4, 5-bisphosphate. J Cell Biol. 2000;150:1299-1310.
54. Higgs HN, Pollard TD. Regulation of actin filament network formation through ARP2/3 complex: activation by a diverse array of proteins. Annu Rev Biochem. 2001;70:649-676.
55. Oda A, Miki H, Wada I, et al. WAVE/Scars in platelets. Blood. 2005;105:3141-3148.
56. Welch MD. The world according to Arp: regulation of actin nucleation by the Arp2/3 complex. Trends Cell Biol. 1999;9:423-427.
57. Glogauer M, Hartwig J, Stossel T. Two pathways through Cdc42 couple the N-formyl receptor to actin nucleation in permeabilized human neutrophils. J Cell Biol. 2000;150:785-796.
58. Sabri S, Jandrot-Perrus M, Bertoglio J, et al. Differential regulation of actin stress fiber assembly and proplatelet formation by alpha2beta1 integrin and GPVI in human megakaryocytes. Blood. 2004;104:3117-3125.

2006 107: 3868-3875
doi:10.1182/blood-2005-07-2755 originally published online January 24, 2006

Characterization of the megakaryocyte demarcation membrane system and its role in thrombopoiesis

Harald Schulze, Manav Korpal, Jonathan Hurov, Sang-We Kim, Jinghang Zhang, Lewis C. Cantley, Thomas Graf and Ramesh A. Shivdasani

Blood (print ISSN 0006-4971, online ISSN 1528-0020), is published weekly by the American Society of Hematology, 2021 L St, NW, Suite 900, Washington DC 20036.